Cepharanthine ameliorates dextran sulphate sodium-induced colitis through modulating gut microbiota

Hong-Gang Wang,[†] Min-Na Zhang,[†]
Xin Wen,[†] Le He, Meng-Hui Zhang,
Jia-Ling Zhang and Xiao-Zhong Yang*
*Department of Gastroenterology, The Affiliated Huaian
No. 1 People's Hospital of Nanjing Medical University,
Huai'an, China.*

Summary

Cepharanthine (CEP) is an active alkaloid isolated from Stephania Cepharantha Hayata. It is reported that the anti-inflammatory properties of CEP could be employed to treat a variety of diseases. In this study, we first found that CEP ameliorates ulcerative colitis (UC) induced by DSS. The effect of CEP on gut microbiota was further evaluated by 16S rRNA gene sequencing, antibiotic pretreatment and faecal microbiota transplantation (FMT). Results showed that the abundances of gut microbiota, such as *Romboutsia*, *Turicibacter* and *Escherichia-Shigella* (especially *Romboutsia*), were significantly reduced after CEP treatment. Additionally, we explored the mechanisms of CEP by a strategy integrating transcriptomics with network pharmacology. The transcriptome data confirmed that CEP functioned through cytokine and cytokine receptor pathways. The expression levels of 10 pro-inflammatory hub genes (such as CXCL1, CXCL9, CCL7) were positively correlated with the abundance of *Romboutsia*. Our data identified *Romboutsia* as a potential pathobiont in UC. Collectively, we confirmed that CEP relieved colon inflammation by modulating gut microbiota and pro-inflammatory cytokine expression. CEP can be adopted to design novel effective therapeutic strategies for UC.

Introduction

Inflammatory bowel disease (IBD), an immune-related chronic bowel inflammatory disease of unknown aetiology, is classified into UC and Crohn's disease (CD) (Argollo *et al.*, 2019). The incidence and prevalence of IBD have kept increasing worldwide, especially in China (Feuerstein *et al.*, 2020). UC, the primary type of IBD, is clinically manifested with recurrent diarrhoea, mucus-relieving bloody stools and abdominal pain (Chang, 2020). UC can be treated with aminosalicylic acid preparations, glucocorticoids, immunosuppressive agents and biological agents (Ungaro *et al.*, 2017). However, the disease may still recur, which makes it urgent to develop new medicine.

Cepharanthine is an active alkaloid isolated from Stephania cepharantha Hayata (Semwal *et al.*, 2010). In Japan, Cepharanthine has a history of more than 70 years in treating radiation-related leukopenia (Kanamori *et al.*, 2016), venomous snakebites (Hifumi *et al.*, 2013), alopecia areata (Hon and Leung, 2011) and other pathologies. In addition, Cepharanthine displays various bioactivities, including anti-inflammation (Huang *et al.*, 2014), anti-tumour (Shahriyar *et al.*, 2018) and immune-modulation (Yamazaki *et al.*, 2017). The anti-inflammatory potential of Cepharanthine can be exploited to treat an array of diseases, such as mastitis (Ershun *et al.*, 2014), acute lung injury (Kao *et al.*, 2015) and cerebral ischaemia/reperfusion injury (Zhao *et al.*, 2020). Studies have found that Cepharanthine acts on the gut microbiota to enhance the therapeutic effect of Cis-diamine-dichloro platinum (CDDP) chemotherapy (Zhou *et al.*, 2019). In this study, relying on the NF-κB pathway, Cepharanthine attenuated inflammation through rescuing intestinal microflora disturbance and up-regulating the relative abundance of some intestinal bacteria, such as *Lactobacillus* (Zhou *et al.*, 2019).

Interestingly, the disruption of gut microbiota and the release of inflammatory cytokines are two major processes in the development of UC. Given that Cepharanthine can protect against inflammation and regulate gut microbiota, this study aimed to explore the underpinning mechanism of Cepharanthine in treating UC based on transcriptomics and network pharmacology.

Results

Cepharanthine ameliorates DSS-induced ulcerative colitis in mice

From the fifth day, the weight loss in the CEP group was significantly less than that in the DSS group ($P < 0.05$) (Fig. 1A). We used the DAI score to quantify the changes in weight, diarrhoea and hematochezia symptoms of mice (Fig. 1B). The DAI score suggested that Cepharanthine reduced the severity of DSS-induced colitis. Furthermore, we found that the colon length of mice was significantly shortened after DSS administration. In contrast, the colon length increased after Cepharanthine treatment and closed to that in the CON group (Fig. 1C and D). H&E staining of the distal colon showed tissue sections from normal mice with normal structures and without inflammatory activity (Fig. 1E). In contrast, the colonic mucosa from the DSS group developed severe inflammatory lesions, including loss of colonic epithelium, disruption of crypt glands and massive inflammatory cell infiltration. However, Cepharanthine notably ameliorated colon inflammation, as manifested by relative intact epithelium cells, the complete structure of the crypt gland and less inflammatory cell infiltration. Consistently, the histopathological score increased in the DSS group ($P < 0.05$), but decreased in the CEP group ($P < 0.05$). Additionally, we also explored whether only Cepharanthine treatment affected the physiological state and colon tissue of normal mice by oral gavage of cepharanthine for seven consecutive days. The results showed that compared with the Control group, CEP-only treatment had no significant effect on the weight loss and colon length of the mice (Fig. S1A–C). H&E staining also confirmed that the morphology and structure of the mice colon tissue between two groups were similar, and no apparent changes were observed (Fig. S1D). The tissue histology score also showed no significant differences between the two groups (Fig. S1E). In summary, these results showed that Cepharanthine inhibits gut inflammation induced by DSS.
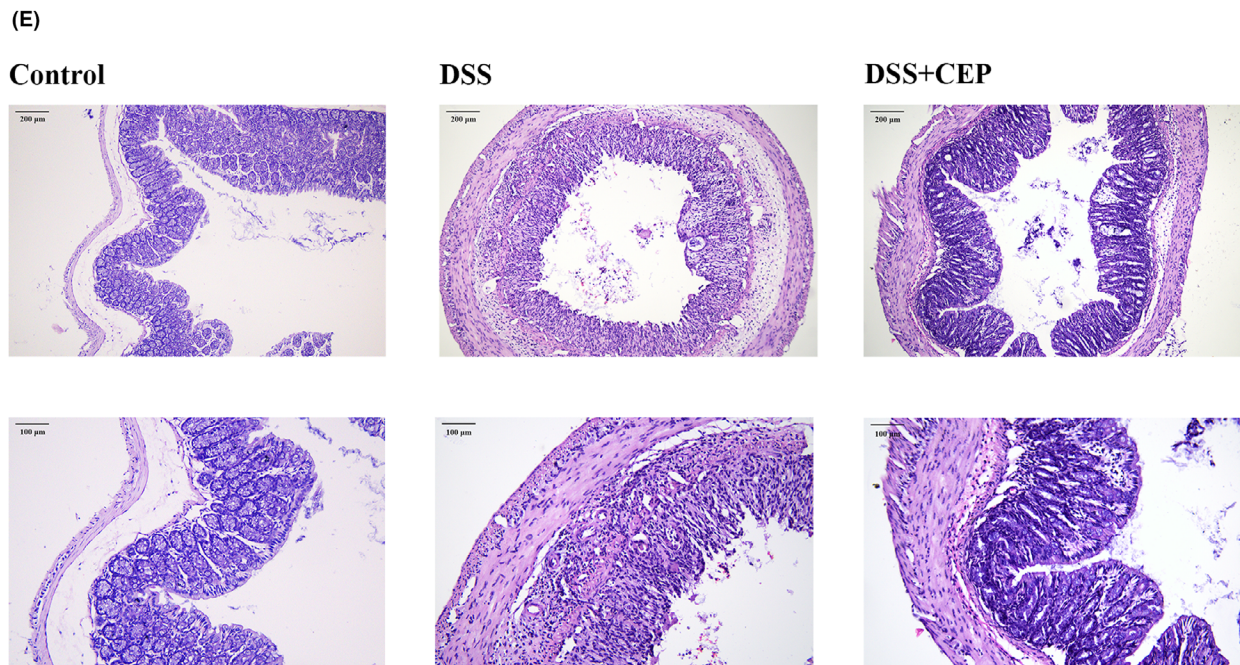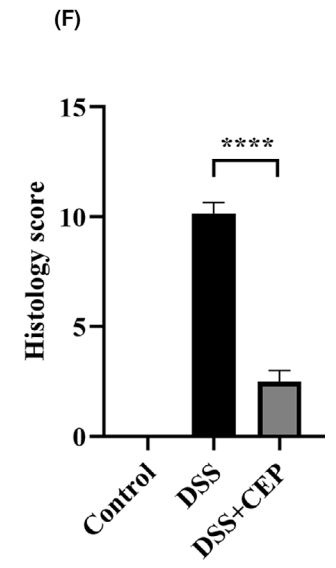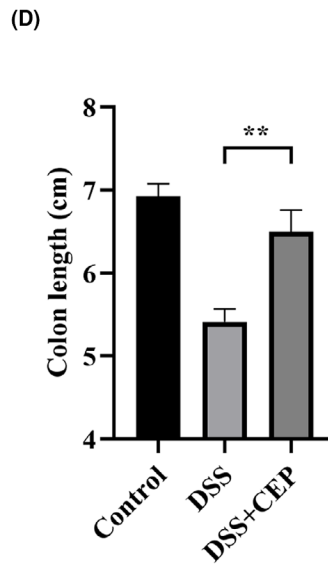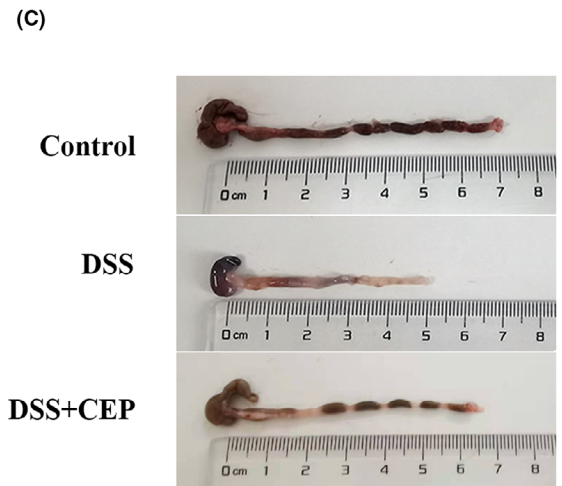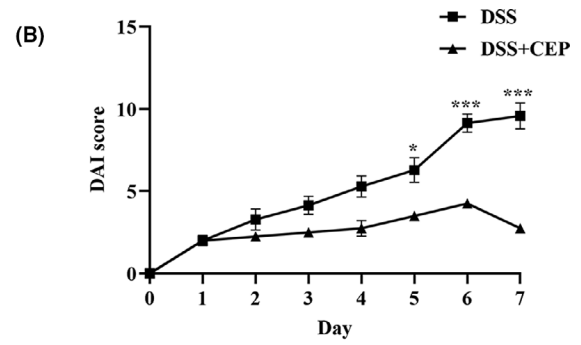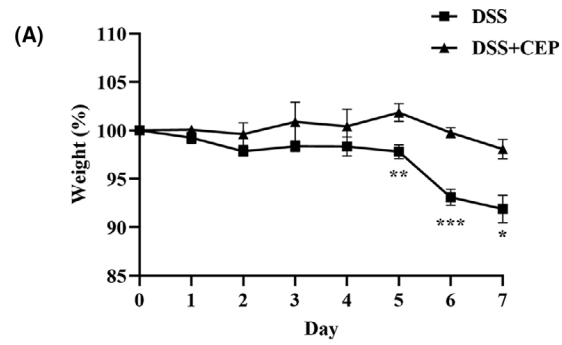
Cepharanthine optimizes the structure of gut microbiota in DSS-induced colitis

To further explore the inhibitory effect of Cepharanthine on gut inflammation, we analysed the data from 16S rRNA-sequencing of faecal samples from different groups. The Venn diagram was used to showcase the overlap of OTUs in faecal microbiota among groups (Fig. 2A); the three groups shared 580 OTUs among gut microbiota: 94 OTUs shared by CEP and DSS groups, 140 OTUs shared by CEP and CON groups, 105 OTUs shared by the DSS and CON groups. As to gut microbiota structure, the CEP group was closer to the CON group than the DSS group. PCA analysis based on OTU abundance showed that the points in the DSS group scattered in the right, which indicated that the microbial structure in the DSS group had undergone a tremendous change than that in the normal group. However, in the CEP group and the normal group, the points clustered in the left, which showed that Cepharanthine could promote the structural recovery of gut microbiota. The microbial structure in the CEP group was more similar to that in the CON group (Fig. 2B). Alpha diversity analysis of gut microbiota showed that compared with that in the DSS group, the Chao 1 index in the CEP group increased ($P < 0.05$), but showed no difference in the CON group (Fig. 2C). The above results indicated that the richness of gut microbiota in CEP-treated mice was closer to that in mice. However, there was no significant difference in the Shannon index between the CEP and DSS groups (Fig. 2D). Therefore, the impact of CEP treatment on the diversity of microbiota was still limited.

At the phylum level, nine bacterial phyla were identified in all samples, topped by *Firmicutes*, *Bacteroidetes*, *Proteobacteria* and *Verrucomicrobia* (Fig. 2E). However, Cepharanthine had a limited effect on their relative abundances ($P > 0.05$). At the genus level, compared with those in the CON group, the abundances of *Escherichia-Shigella*, *Romboutsia* and *Turicibacter* increased significantly, whereas that of Ruminococcus_1 was decreased considerably in the DSS group (Fig. 2F). Interestingly, Cepharanthine dramatically reduced the relative abundances of *Romboutsia*, *Turicibacter* and *Escherichia-Shigella* ($P < 0.05$), till close to those in the CON group. Conversely, the abundances of *Family_XIII_AD3011_group*, *Acetatifactor* and *Ruminococcaceae_N-K4A214_group* increased significantly ($P < 0.05$) after treatment with Cepharanthine (Fig. 2G). Subsequent LEfSe analysis showed substantial differences in *Romboutsia*, *Escherichia-Shigella* and *Turicibacter* in the DSS group, which indicated that these genera are associated with the activity of UC (Fig. 2H). Notably, Cepharanthine significantly reduced the abundance of these genera. Furthermore, we screened the gut microbes with generic differences between the DSS and Cepharanthine groups by Metastats analysis. We found that *Romboutsia* had the most significant generic differences between the two

---

Fig. 1. CEP treatment ameliorates DSS-induced colitis in Mice. (A) the percentage of the weight of mice was measured for 7 days; (B)The DAI score; (C) Photographs of the colon; (D) The colon length; (E) H&E staining for colon tissues. (100×; 200×) (F) The Histology score; Values are presented as the mean ± standard error of the mean (SEM); CON group, $n = 7$; DSS group, $n = 7$; DSS + CEP group, $n = 4$; *$P < 0.05$, **$P < 0.01$, ***$P < 0.001$.
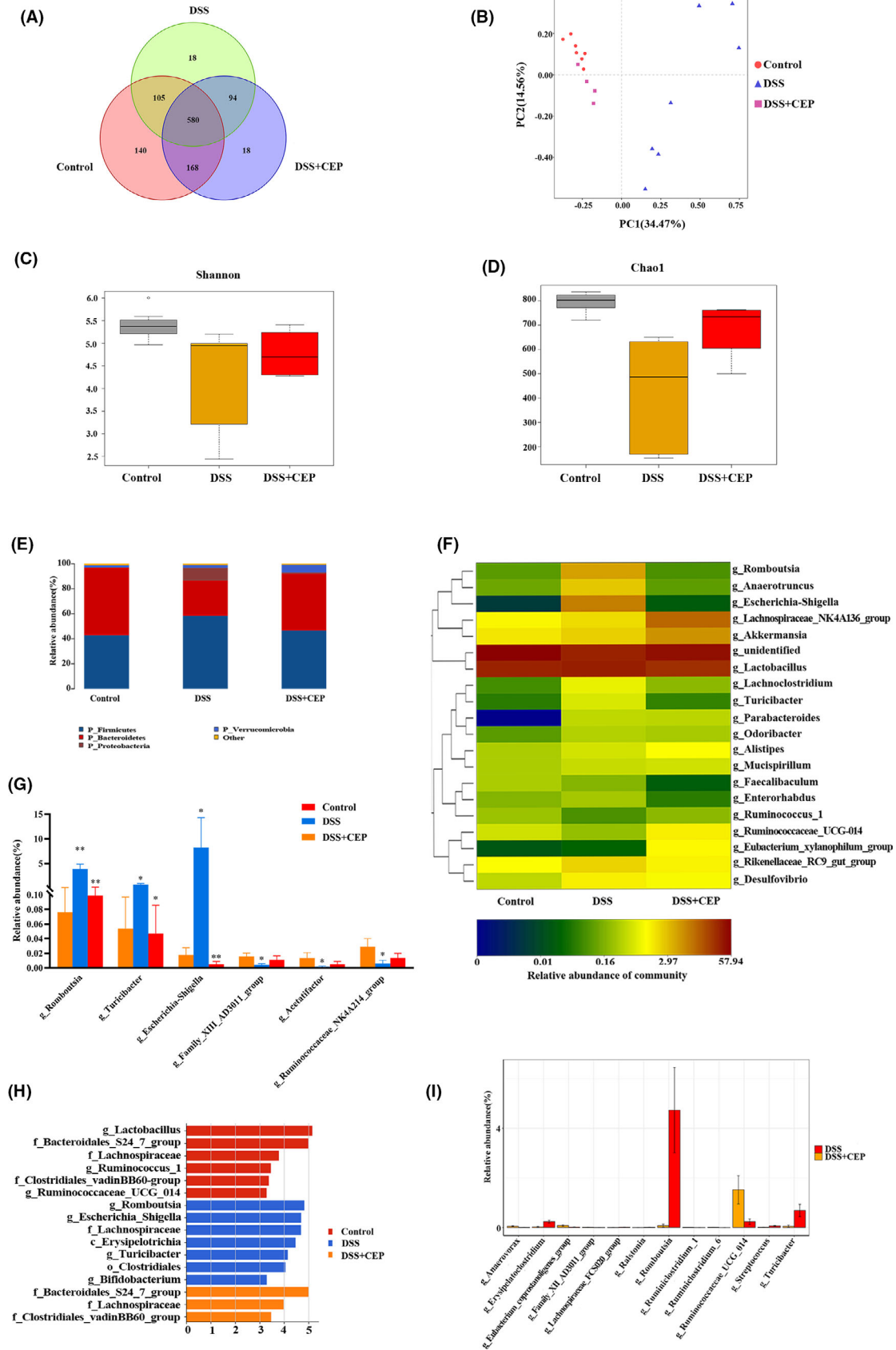
Fig. 2. Cepharanthine regulates the structure and composition of gut microbiota. (A)The Venn diagram of CON, DSS, and DSS + CEP group; (B) PCoA score (C) Chao index (D) Shannon index; (E) Bar chart of gut microbiota at the phylum level; (F) Heatmap of gut microbiota at the genus level; (G) Relative abundance of discriminative gut microbiota at the genus level; (H) The LEfSe analysis; (I) The metastats analysis between DSS and DSS + CEP group; Values are presented as the mean $\pm$ standard error of the mean (SEM); CON group, $n = 7$; DSS group, $n = 7$; DSS + CEP group, $n = 4$; *$P < 0.05$, **$P < 0.01$, ***$P < 0.001$.

groups (Fig. 2I). We speculated that the effect of Cepharanthine on DSS-induced colitis might be related to the abundance of *Romboutsia*. The above results revealed that Cepharanthine could optimize gut microbiota structure in DSS-induced colitis.

Faecal microbiota transplantation treatment ameliorates intestinal inflammation by regulating the gut microbiota

To confirm that Cepharanthine ameliorates colitis through modulating gut microbiota, we collected the mouse faecal microbiota after Cepharanthine administration and used them to treat DSS-induced colitis in mice. As shown in Fig. 3A, the weight loss in the mice receiving FMT was less than that in the DSS group. DAI scores also showed that the colonic colitis in the FMT group was alleviated (Fig. 3B). We further compared the severity of colonic inflammation by H&E staining at the pathological level. As shown in Fig. 3C, compared with the DSS group, the FMT group presented complete colonic epithelial tissue, more normal crypt glands and less infiltration of inflammatory cells. In addition, the histological score in the FMT group was also significantly lower than that in the DSS group (Fig. 3D). Colon length is another indicator to assess the degree of gut inflammation. However, there was no statistical difference in colon length between the two groups, because of the limited sample size (Fig. 3E and F).

We also sequenced the faecal samples to compare the gut microbiota between the DSS group and the FMT-treated group. The results showed that FMT treatment restored microbiota dysbiosis. At the phylum level, *Firmicutes* and *Bacteroides* dominated in both two groups. After FMT, there was a significant increase in *Actinobacteria* and a decrease in *Tenericutes* (Fig. 4A). At the genus level, FMT significantly decreased the levels of *Romboutsia, Tyzzerella, Oscillibacter, Faecalibaculum, Lactobacillus*, compared with those in the DSS group. In addition, FMT could dramatically increase the relative abundance of *Lactobacillus* (Fig. 4B and C).

These results confirmed that Cepharanthine countered colitis through modulating gut microbiota.

Effects of antibiotics pretreatment on the cepharanthine-treated colitis

To further clarify the beneficial role of Cepharanthine in treating colitis, we pretreated the mice with broad-spectrum antibiotics (vancomycin, colistin, neomycin and metronidazole) one week in advance to disrupt the status of gut microbiota (Fig. 5A). After that, two groups were administrated with 2.5% DSS for 7 days, while the Abx + DSS + CEP group was treated with oral 10 mg kg^{-1} Cepharanthine. We found that the weight of mice in the group decreased significantly compared with that in the Abx + DSS group (Fig. 5B). Next, we used the DAI score to assess the degree of intestinal inflammation in two groups. As shown in Fig. 5C, there was no statistical difference in DAI score between both groups. At the end of modelling, we found that the colon length in the Abx + DSS + CEP group was similar to that in the Abx + DSS group (Fig. 5D). H&E staining revealed that the inflammatory infiltration of the intestinal epithelium in the Abx + DSS + CEP group was similar to that in the Abx + DSS group (Fig. 5E). Similarly, the histological score also revealed no significant difference in the degree of colon tissue damage between the two groups (Fig. 5F). These results indicated that Cepharanthine posed no apparent therapeutic effect on UC after the gut microbiota were disrupted.

Cepharanthine functions through the cytokine-cytokine receptor interaction pathway

We performed transcriptome sequencing on colon tissue samples. The results showed 714 differentially expressed genes (DEGs) between the DSS group and CEP group ($P_{adj} \leq 0.05$), including 494 down-regulated and 220 up-regulated (Fig. 6A). GO enrichment analysis showed that the differentially expressed genes were most enriched in binding (Fig. 6B). Next, KEGG pathway enrichment analysis showed that these DEGs were involved in 20 pathways, including cytokine–cytokine receptor interaction, chemokine signalling pathway, TNF signalling pathway (Fig. 6C). The cytokine–cytokine receptor interaction pathway was the most enriched. Next, 108 prominent DEGs were screened out according to |log2foldchange| >2 and $P_{adj} < 0.01$, and used to construct a PPI network using Search Tool for the Retrieval of Interacting Genes (STRING 11.5; https://string-db.org/). Among its 75 nodes and 527 edges (Fig. 6D), the most significant modules (18 nodes, 145 edges and a score of 17.059) were recognized by the MCODE plug of Cytoscape (Fig. 6E). The KEGG enrichment pathway analysis was repeated, revealing that 15 DEGs were
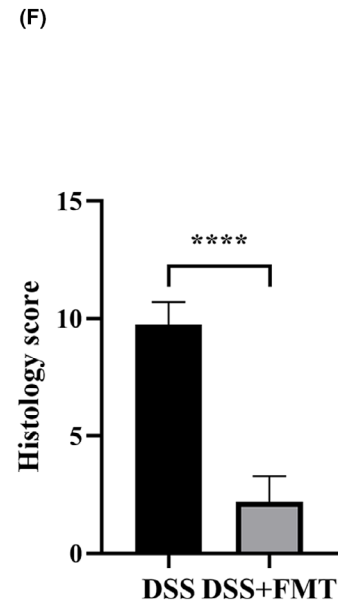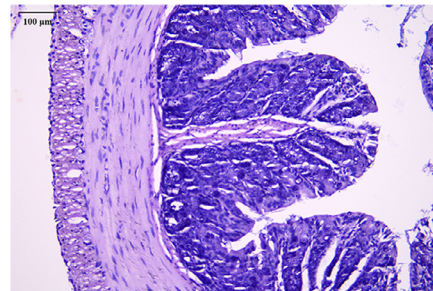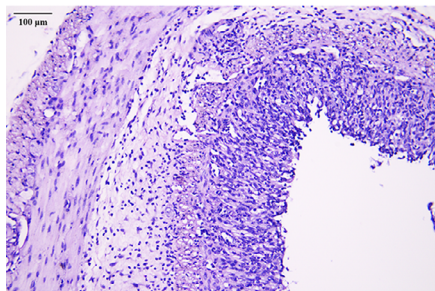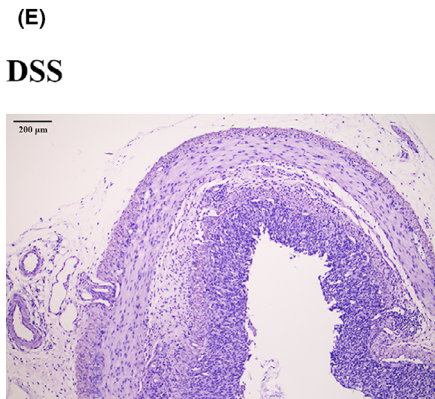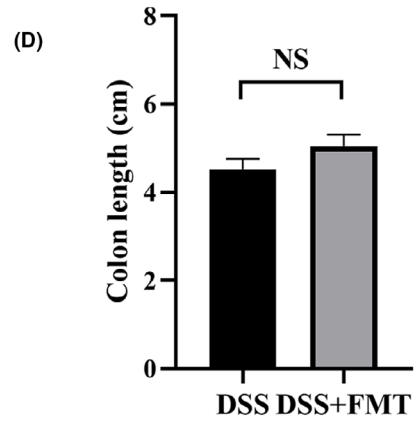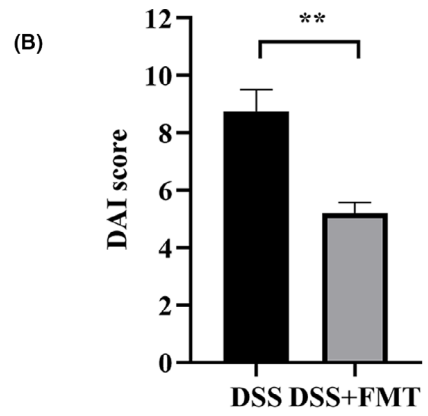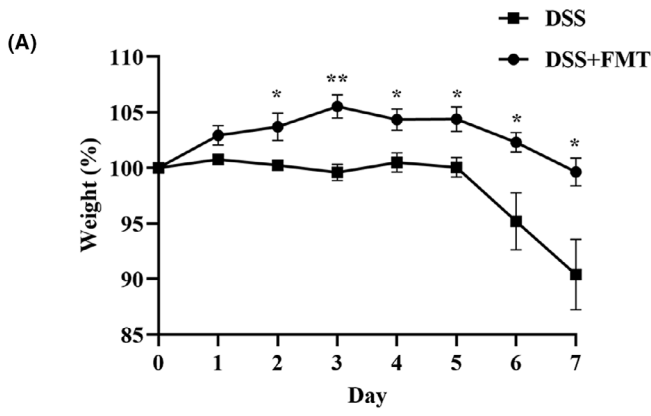
Fig. 3. FMT treatment ameliorates intestinal inflammation by regulating the gut microbiota. (A) the percentage of the weight of mice was measured for 7 days; (B)The DAI score; (C) Photographs of the colon; (D) The colon length; (E) H&E staining for colon tissues. (100×; 200×) (F) The Histology score; Values are presented as the mean ± standard error of the mean (SEM); DSS group, $n = 4$; DSS + FMT group, $n = 5$; *$P < 0.05$, **$P < 0.01$, ***$P < 0.001$.
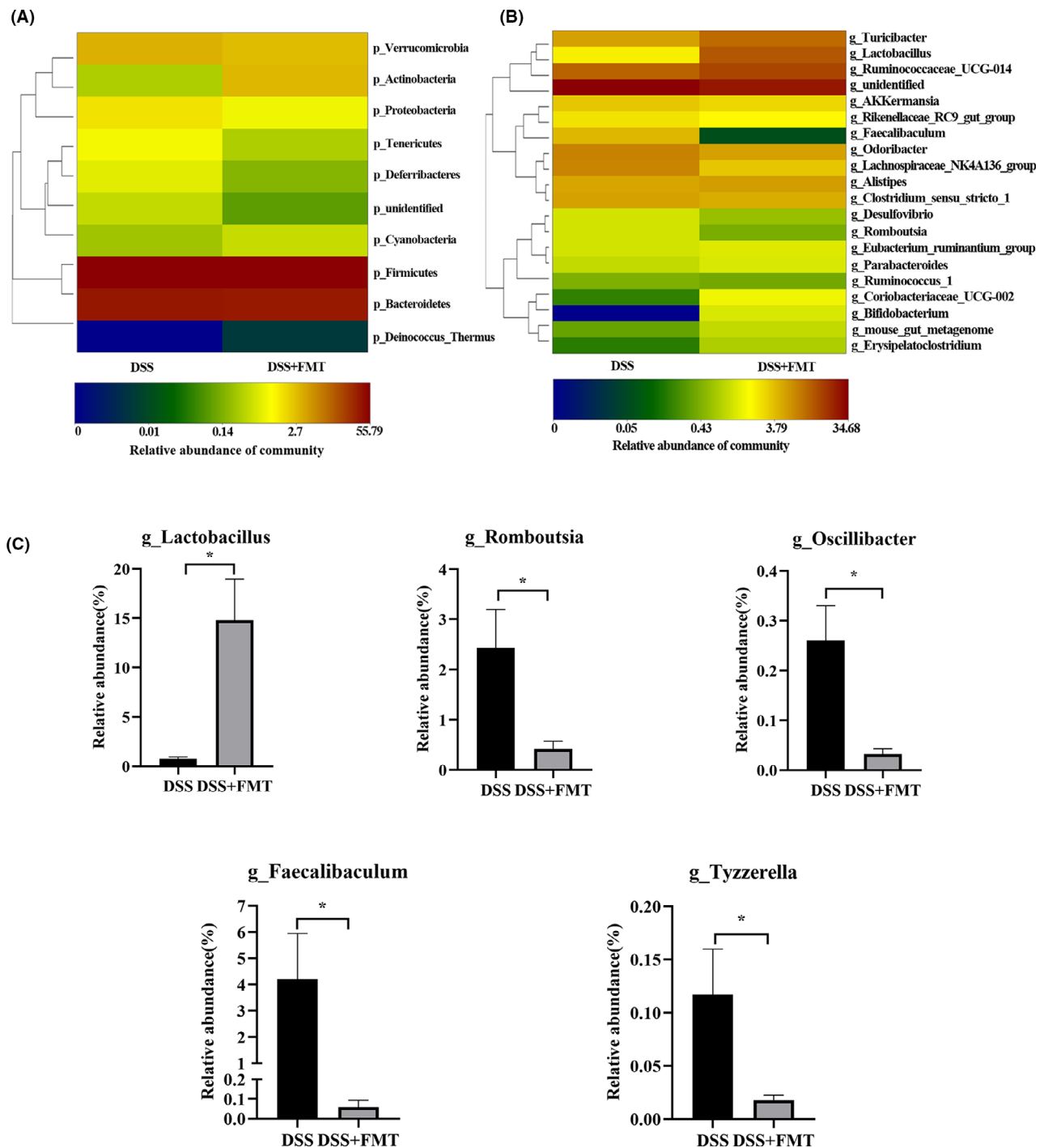
Fig. 4. (A) Heatmap of gut microbiota at the phylum level; (B) Heatmap of gut microbiota at the genus level; (C) Relative abundance of discriminative gut microbiota at the genus level; *$P < 0.05$.

(A)

(B)

(C)

(D)

(E)

(F)
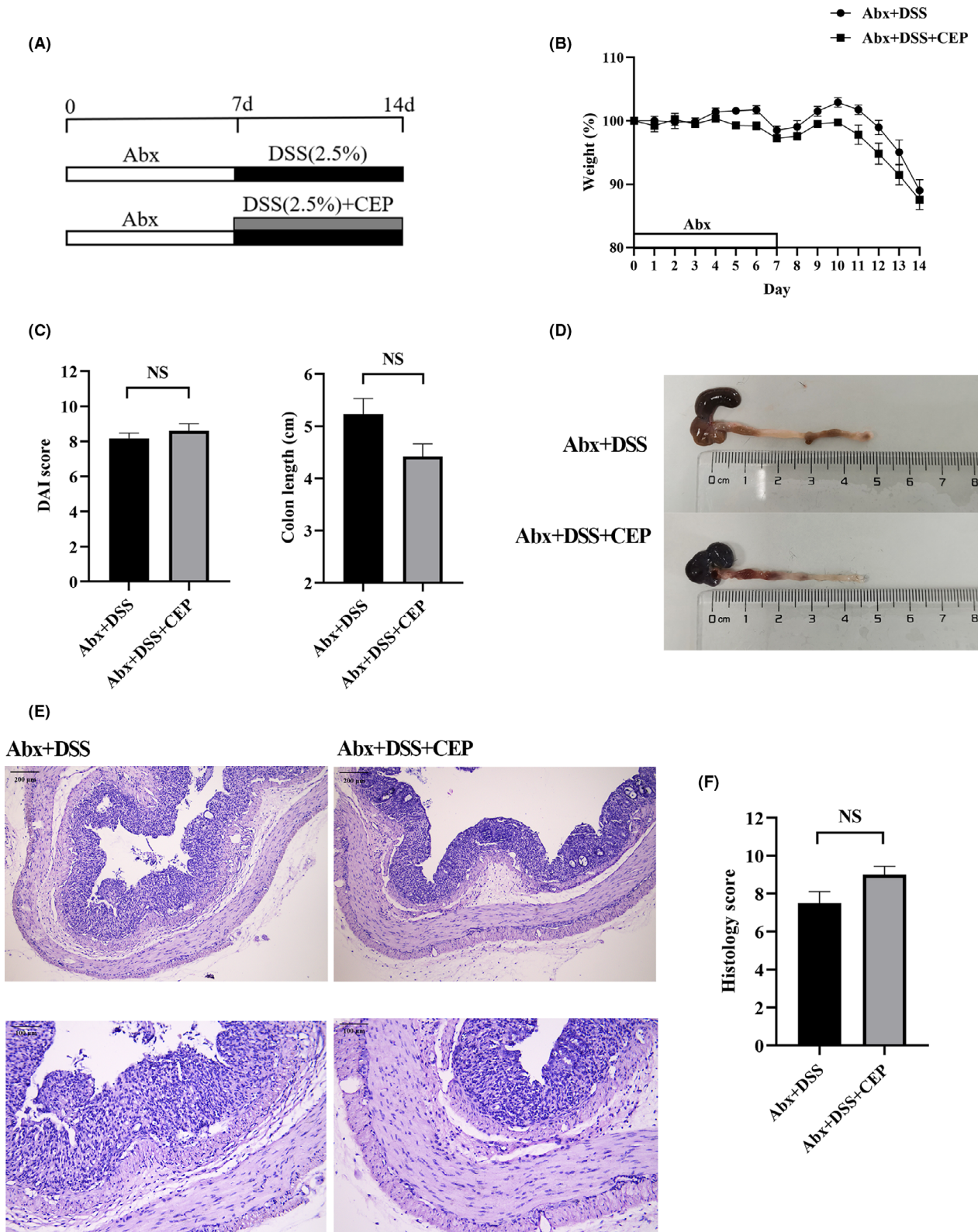
Fig. 5. Effects of Abx pretreatment on the CEP-treated colitis. (A) Treatment diagram of Abx + DSS and Abx + DSS + CEP group; (B) the percentage of the weight of mice was measured for 7 days; (C)The DAI score; The colon length; (D) Photographs of colon; (E) H&E staining for colon tissues. (100×; 200×) (F) The Histology score; Values are presented as the mean ± standard error of the mean (SEM); $n = 6$ for each treatment. *$P < 0.05$, **$P < 0.01$, ***$P < 0.001$.

Fig. 6. CEP affects Cytokine-cytokine receptor interaction pathways. (A) Volcano plot analysis identifies DEGs between DSS and DSS + CEP group; (B) Go term enrichment analysis of DEGs; (C) KEGG pathway analysis of DEGs. Correlation analysis between gut microbiota and significant genus. (D) String software analyzed the protein-protein network; (E) The most significant module identified by MCODE (score = 17.059). (F) The spearman's correlation analysis between the DEGs and Romboutsia genus by SPSS software.

Table 1. KEGG pathway enrichment analysis of 18 core genes (*P* < 0.05).

Term	Count%	Genes
Cytokine–cytokine receptor interaction	15	CCL12, CXCL9, CSF3, CXCL1, TNF, CXCL5, CXCL10, IL6, IFNG, CCL7, IL1B, CXCR3, CCL4, CXCR2, CCL2.
Chemokine signalling pathway	11	CXCL10, CXCL9, CCL12, CCL7, CXCR3, CXCR2, CCL4, CCL2, CXCL1, CXCL3, CXCL5.
Malaria	7	IL6, CCL12, CSF3, IFNG, IL1B, CCL2, TNF.
TNF signalling pathway	8	CXCL10, IL6, CCL12, IL1B, CCL2, CXCL1, CXCL3, TNF.
Rheumatoid arthritis	7	IL6, CCL12, IFNG, IL1B, CCL2, TNF, CXCL5.
Influenza A	8	IL33, CXCL10, IL6, CCL12, IFNG, IL1B, CCL2, TNF.
NOD-like receptor signalling pathway	6	IL6, CCL12, IL1B, CCL2, CXCL1, TNF.
Salmonella infection	6	IL6, IFNG, IL1B, CCL4, CXCL1, CXCL3.
Toll-like receptor signalling pathway	6	CXCL10, IL6, CXCL9, IL1B, CCL4, TNF.
Chagas disease	6	IL6, CCL12, IFNG, IL1B, CCL2, TNF.
Legionellosis	5	IL6, IL1B, CXCL1, CXCL3, TNF.
Cytosolic DNA-sensing pathway	5	IL33, CXCL10, IL6, IL1B, CCL4.
African trypanosomiasis	4	IL6, IFNG, IL1B, TNF.
Herpes simplex infection	6	IL6, CCL12, IFNG, IL1B, CCL2, TNF.
Graft-versus-host disease	4	IL6, IFNG, IL1B, TNF.
Inflammatory bowel disease	4	IL6, IFNG, IL1B, TNF.
Pertussis	4	IL6, IL1B, TNF, CXCL5.
Hematopoietic cell lineage	4	IL6, CSF3, IL1B, TNF.
Amoebiasis	4	IL6, IFNG, IL1B, TNF.
Tuberculosis	4	IL6, IFNG, IL1B, TNF.
Type I diabetes mellitus	3	IFNG, IL1B, TNF.
Leishmaniasis	3	IFNG, IL1B, TNF.
NF-kappa B signalling pathway	3	IL1B, CCL4, TNF.
HIF-1 signalling pathway	3	IL6, IFNG, TIMP1.
Osteoclast differentiation	3	IFNG, IL1B, TNF.
Measles	3	IL6, IFNG, IL1B.
Jak-STAT signalling pathway	3	IL6, CSF3, IFNG.
Non-alcoholic fatty liver disease	3	IL6, IL1B, TNF.

markedly enriched in the cytokine–cytokine interaction and chemokine signalling pathways (Table 1).

Correlation analysis between gut microbiota and 15 DEGs

We analysed the correlation between the aforementioned 15 DEGs and *Romboutsia* (Fig. 6F). Interestingly, the results showed that 10 of 15 genes were positively correlated with the relative abundance of *Romboutsia* (*P* < 0.05), including Cxcl1, Cxcl9, Ccl7, Il6, Ccl2, Il1β, Cxcr2, Ccl12 and Tnf. Subsequently, our qRT-PCR analysis verified that Cxcl1, Ccl7, Ccl2, IL6 and IL1β expression was upregulated in the DSS group, then downregulated after CEP treatment (Fig. S2). The results of qRT-PCR were consistent with the sequencing data.

Discussion

Increasing plant-derived bioactive alkaloids have been discovered to have therapeutic effects on UC, such as aloperine (Fu *et al.*, 2017), palmatine (Zhang *et al.*, 2018), neferine (Wu *et al.*, 2018) and berberine (Xiong *et al.*, 2021). Chea *et al.* (2007) reported that oral Cepharanthine (10 mg kg^{-1}) decreased the incidence of parasitemia by 50% in mice. In our study, we for the first-time report that Cepharanthine (10 mg kg^{-1}) could ameliorate UC induced by DSS. Our results provide evidences that Cepharanthine may be used to design new therapeutic strategies for UC.

Inflammatory bowel disease is characterized by immune-related chronic intestinal inflammation driven by genetic, environmental and microbial factors (Imhann *et al.*, 2018). Microbiological mechanisms have been proven indispensable for IBD pathogenesis (Collins and Patterson, 2020). Several studies have reported that the gut microbiota takes on a profile in IBD patients different from that in healthy individuals (Jonkers *et al.*, 2012; Marchesi *et al.*, 2016). In our study, DSS induced a significant reduction in microbial alpha and beta diversity (Fig. 2A–D), and Cepharanthine attenuated this reduction. However, the impact of Cepharanthine on the composition of gut microbiota was more profound. At the genus level, DSS administration increased the levels of *Escherichia-Shigella*, *Romboutsia* and *Turicibacter*, while Cepharanthine significantly reduced their abundance. A study reported that compared with those in non-inflamed mucosae, the generic abundance of *Escherichia-Shigella* increased in the inflamed mucosae in UC patients (Hold *et al.*, 2014), suggesting that *Escherichia-Shigella* may be a potential pathogenic genus. In addition, *Turicibacter*

is a genus in the *Firmicutes* phylum that produces lactic acid by fermenting sugars and is commonly detected in the guts of animals. It has reported an increase in the abundance of *Turicibacter* in the RA (Rheumatoid arthritis, RA), an immune-mediated inflammatory disease (Chen *et al.*, 2016). The abundance of *Turicibacter* is positively correlated with the level of pro-inflammatory cytokines in DSS-induced colitis (Liang *et al.*, 2019). Furthermore, LEfse (Linear discriminant analysis Effect Size, LEfse) analysis showed that *Romboutsia* in the DSS group differed significantly from that in the other two groups. The Metastats analysis also showed that the generic level of *Romboutsia* presented the most evident difference between the DSS and CEP groups. *Romboutsia* is an obligate anaerobe in the intestine, belonging to *Firmicutes* phylum, and its abundance increases in various diseases, such as neurodevelopmental disorders (Bojovic *et al.*, 2020), depression (Zheng *et al.*, 2021), irritable bowel syndrome (Enqi *et al.*, 2020), gastric cancer (Zhang *et al.*, 2021). A study has shown that the relative abundance of *Romboutsia* is correlated with circulating inflammatory (IL-1β) and anxiety-like behaviour (Grant *et al.*, 2021). The relative abundance of *Romoutsia* also increased in DSS-induced colitis in the study of Wu *et al.* (2021), which is consistent with our findings.

Furthermore, we utilized FMT to confirm the therapeutic effect of Cepharanthine in UC. Our results showed that FMT alleviated colonic inflammation, as manifested by the positive changes in weight change, DAI scores and colon length compared with those in the DSS group. The histopathological assessment demonstrated that the inflammatory cell infiltration, loss of crypts and destruction of the colon wall were inhibited in the FMT group. These results indicate that Cepharanthine modulates the gut microbiome to control UC. After broad-spectrum antibiotics were used in advance to destroy the gut microbiota of mice, we observed that Cepharanthine was not as effective as before. These results infer those antibiotics may disrupt the gut microbiota restored by Cepharanthine, thus discounting the efficacy of Cepharanthine. These results once again prove that Cepharanthine ameliorates colitis by regulating gut microbiota.

Next, to further explore the mechanism of Cepharanthine in treating UC, 714 DEGs were identified between the Cepharanthine group and the DSS group based on the high-throughput RNA sequencing data. Moreover, KEGG pathway enrichment analysis showed that these DEGs were most enriched in cytokine–cytokine receptor interaction, which was significantly suppressed by Cepharanthine. Then, the expression of 10 hub genes was decreased and positively correlated with the level of *Romboutsia* in the treatment with Cepharanthine, including Cxcl1, Cxcl9, Ccl7, IL6, Ccl2, IL1β,

Cxcr2, Cxcl5, Ccl12 and Tnf. Cxcl1 has been considered as an IBD-relevant proinflammatory cytokine. Shen S *et al* have reported that CXCL1 can recruit neutrophils in an autocrine manner and aggravate intestinal inflammation (Shen *et al.*, 2018). CXCL9 also plays a significant role in recruiting mononuclear cells and granulocytes. CXCL9 mRNA level in the colonic mucosa of IBD is higher than that in the healthy controls (Hosomi *et al.*, 2011). CXCL5 expression increases significantly in IBD patients as compared to that in healthy donors, but its role in the pathogenesis of UC remains to be explored. FBXW7/EZH2/CCL2/CCL7 serves as a critical axis in intestinal inflammation (He *et al.*, 2019). CCL12 (MCP-5) is expressed mainly in recruited inflammatory macrophages and has been implicated in B cell activation (Iijima *et al.*, 2011). Chronic mucosal inflammation of IBD is related to abnormal B cell function (Brandtzaeg *et al.*, 2006). Several studies suggest the tumour necrosis factor (TNF) is correlated with mucosal inflammatory involvement in the pathogenesis of IBD (Billmeier *et al.*, 2016). In this study, we found that these DEGs participated in the pro-inflammatory mechanism of UC and that *Romboutsia* played a pro-inflammatory role in UC.

In conclusion, we for the first time found that Cepharanthine ameliorates gut inflammation by correcting gut microbiota dysbiosis in DSS-induced colitis. The abundance of *Romboutsia* is correlated with the efficacy of Cepharanthine. Our findings offer a possibility of treating colitis by modulating gut microbiota with Cepharanthine.

Experimental procedures

Ethics approval

All animal experiments were approved by the Laboratory Animal Welfare and Ethics committee of Nanjing Medical University.

Animals and reagents

Seven-week-old female C57BL/10 mice were purchased from the Model Animal Research Center of Nanjing University. All mice were housed in the experimental animal centre of Huai'an NO.1 People's Hospital Affiliated to Nanjing Medical University under a 12 h light/dark cycle at an environmental temperature of $21 \pm 2°C$ and humidity of $45 \pm 10\%$, with free access to sterilized standard rodent chow food and water. All animal experiments were performed by the principles outlined by the National Institutes of Health Guide for Care and Use of Laboratory Animals. The mice were acclimatized to the new environment for at least 1 week before the start of the experiment. Dextran sulphate sodium (DSS, the molecular weight of 36–50 kDa) was purchased from

MP Biomedicals LLC. Cepharanthine was purchased from Chengdu Biopurify Phytochemicals (Sichuan, China).

Animal grouping

The mice were randomly divided into control (CON), DSS and DSS + Cepharanthine (CEP) groups. The mice from the CEP and DSS groups were given distilled water containing 2.5% DSS(w/v) for 7 days. Meanwhile, the mice from the CEP group received Cepharanthine dissolved in distilled water via intragastric gavage from day 1 to day 7 (daily, 10 mg kg^{-1} Cepharanthine). Cepharanthine of 10 mg kg^{-1} has been proven as a safe dose in animal studies (Ershun *et al.*, 2014).

Disease activity indexes

DAI score was calculated by a 0–4 scale based on the following parameters: body weight loss (1, 1–5%; 2, 5–10%; 3, 10–15%; and 4, $\geq$ 15%), stool consistency (0, normal; 2, loose stools; 4, diarrhoea) and blood in the stool (0, no blood seen; 2, apparent blood with stool; 4, grossly bloody stool). Loss of body weight by more than 30% was used as a criterion for humane euthanasia to reduce the pain of the mice.

Histopathological analysis

The mice were sacrificed by cervical dislocation under anaesthesia at the end of the experiment. The colon length was measured, the colon cavity was washed with normal saline and the distal colon tissues were taken for histopathological analysis. The tissue samples were fixed in 4% paraformaldehyde, dehydrated in ethanol and embedded in paraffin. Subsequently, 4-μm sections were prepared and stained with haematoxylin and eosin (H&E). The severity of colon tissue inflammation was scored according to the degrees of inflammation (0, none; 1, mild; 2, moderate; 3, severe), crypt gland damage (0, normal; 1, basal 1/3 damage; 2, basal 2/3 damage; 3, crypt lost and surface epithelium present; 4 crypt and surface epithelium lost), infiltration of lymphocyte (0, 0%; 1, 10%; 2, 10%–25%; 3, 25%–50%; 4, > 50%), structure of colon wall (0, none; 1, mucosa; 2, submucosa; 3, transmural). The total histological score was defined as the sum of all parameter scores (Li *et al.*, 2020).

Faeces preparation and transplantation

Faecal microbiota transplantation was performed as detailed previously with minor changes (Wen *et al.*, 2021). Fresh faecal samples were collected from the CEP group mice, mixed with sterile normal saline to 0.125 g ml^{-1} concentration and homogenized immediately. The homogenate was centrifuged at 1200 rpm for 5 min at 4°C, the supernatant was then removed and the faecal sediment was suspended in sterile normal saline to a concentration of 0.25 g ml^{-1}. The suspension was delivered into normal C57bL/10 recipient mice by intragastric gavage (0.1 ml/10 g) every other day, with care to avoid regurgitation. The recipient mice were still administered with 2.5% (w/v) DSS for 1 week at the same time. Finally, all the mice were euthanized for colon tissue collection.

Antibiotics pretreatment

The mice were randomly divided into two groups: Abx + DSS and Abx + DSS + CEP groups. The antibiotics consisted of vancomycin (50 mg kg^{-1}), ampicillin (100 mg kg^{-1}), metronidazole (100 mg kg^{-1}) and neomycin (100 mg kg^{-1}) as previously reported (Rakoff-Nahoum *et al.*, 2004). Then the antibiotics were mixed with sterile normal saline, and each mouse was given oral gavage (0.2 ml per day, for 7 consecutive days) before the start of the experiment. From day 7, the two groups were simultaneously given distilled water containing 2.5% DSS. The Abx + DSS + CEP group received Cepharanthine dissolved in distilled water via intragastric gavage (daily, from day 7 to day 14).

Gut microbiota analysis

The fresh faecal samples in mice were collected, and the microbial community genomic total DNA was extracted by an E.Z.N.A.® soil DNA Kit (Omega Bio-Tek, Norcross, GA, USA). The NanoDrop 2000 UV-vis spectrophotometer (Thermo Scientific, Wilmington, USA) was used to check the concentration and purity of DNA. Then, the hypervariable V3-V4 regions of the 16SrRNA sequence were then amplified using an ABI GeneAmp® 9700 PCR thermocycler (ABI, CA, USA). The PCR products were purified by the AxyPrep DNA Gel Extraction Kit (Axygen Biosciences, Union City, CA, USA) according to manufacturer's instructions and quantified using Quantus™ Fluorometer (Promega, Madison, WI, USA). Sequencing was performed on an Illumina MiSeq PE300 platform (Illumina, San Diego, CA, USA), and the original data were filtered in the NCBI Sequence Read Archive (SRA).

Transcriptome analysis

Total RNA was extracted from the distal colon tissue samples of the mice. For sample preparation, 2 μg of RNA per sample was used as input material. RNA concentration was assessed using a Nanodrop spectrophotometer

(IMPLEN, CA, USA). RNA integrity was determined by Agilent 2100 (Agilent Technologies, CA, USA). According to the manufacturer's recommendations, the sample libraries were generated using NEBNext UltraTM RNA Library Prep Kit for Illumina (NEB, USA). The library was sequenced using Illumina Hiseq 4000 platform to generate paired-end 150 bp reads. Next, we used Star and Cufflinks software to complete alignment, analyse transcripts and make a quantitative analysis of all genes. To identify DEGs between two samples, the expression level of each transcript was calculated by HTSeq software, using the fragments per kilobase of exon per million mapped reads (FPKM) value of 0.1 or 1 as the threshold for judging whether the gene was expressed. DEGs analysis was performed on the DESeq R package (1.10.1). Additionally, GO enrichment analysis was performed using GOseq software and based on Wallenius non-central hypergeometric distribution. KEGG pathway enrichment analysis was performed using KOBAS software. Rich factor, *q*-value and the number of genes enriched in this pathway were used to measure the degree of KEGG enrichment. Rich factor referred to the ratio of the number of DEGs enriched in the pathway to the number of annotated genes. *Q* value (0–1) was the *P*-value after correction by multiple hypothesis testing.

PPI network

PPI network of DEGs was constructed by Search Tool for the Retrieval of Interacting Genes (STRING; https://string-db.org). Then the PPIs of these DEGs were visualized in Cytoscape software (Cytoscape, 3.7.2), and significant modules in the PPI network were identified by molecular complex detection (MCODE).

Correlation analysis

Correlation analysis between 13 DEGs and *Romboutsia* was performed with the Pearson correlation coefficient by IBM SPSS Statistics 26 program (IBM Corporation, Armonk, NY, USA). Then, these results were visualized in a bioinformatics platform (http://www.bioinformatics.com.cn) and 12 hub genes were screened out according to *P*-value <0.05.

Quantitative real-time PCR (qRT-PCR)

Total RNA was extracted from colon tissues by RNA simple total RNA kit (TIANGEN, DP419). Two micro litres of total RNA were pipetted for measurement by Nanodrop. RNA was then transcribed into cDNA using a PrimeScript™ RT Master Mix kit (TAKARA, Ref. RR036A). qRT-PCR was performed using a LightCycler Instrument. PCR system using SYBR® premix Ex Taq™

(TAKARA, RR420A) following manufacturer's instructions. The primers used are listed in Table S1. The relative mRNA levels were normalized to those of β-actin using the 2-ΔΔCt method.

Statistical analysis

The data were expressed as means ± standard error of the mean (SEM). A *t*-test was performed for comparison between two groups by Graphpad Prism 8.0 software (GraphPad Software Inc., San Diego, CA, USA). $P < 0.05$ (*), $P < 0.01$ (**) and $P < 0.001$ (***) were considered as statistical significance.

Conflict of interest

The authors declare that they have no conflict of interest in this study.

References

Argollo, M., Gilardi, D., Peyrin-Biroulet, C., Chabot, J.F., Peyrin-Biroulet, L., and Danese, S. (2019) Comorbidities in inflammatory bowel disease: a call for action. *Lancet Gastroenterol Hepatol* **4:** 643–654.

Billmeier, U., Dieterich, W., Neurath, M.F., and Atreya, R. (2016) Molecular mechanism of action of anti-tumor necrosis factor antibodies in inflammatory bowel diseases. *World J Gastroenterol* **22:** 9300–9313.

Bojovic, K., Ignjatovic Eth, I., Sokovic Bajic, S., Vojnovic Milutinovic, D., Tomic, M., Golic, N., and Tolinacki, M. (2020) Gut microbiota dysbiosis associated with altered production of short chain fatty acids in children with neurodevelopmental disorders. *Front Cell Infect Microbiol* **10:** 223.

Brandtzaeg, P., Carlsen, H.S., and Halstensen, T.S. (2006) The B-cell system in inflammatory bowel disease. *Adv Exp Med Biol* **579:** 149–167.

Chang, J.T. (2020) Pathophysiology of inflammatory bowel diseases. *N Engl J Med* **383:** 2652–2664.

Chea, A., Hout, S., Bun, S.-S., Tabatadze, N., Gasquet, M., Azas, N., *et al.* (2007) Antimalarial activity of alkaloids isolated from *Stephania rotunda*. *J Ethnopharmacol* **112:** 132–137.

Chen, J., Wright, K., Davis, J.M., Jeraldo, P., Marietta, E.V., Murray, J., *et al.* (2016) An expansion of rare lineage intestinal microbes characterizes rheumatoid arthritis. *Genome Med* **8:** 43.

Collins, S.L., and Patterson, A.D. (2020) The gut microbiome: an orchestrator of xenobiotic metabolism. *Acta Pharm Sin B* **10:** 19–32.

Enqi, W., Jingzhu, S., Lingpeng, P., and Yaqin, L. (2020) Comparison of the gut microbiota disturbance in rat models of irritable bowel syndrome induced by maternal separation and multiple early-life adversity. *Front Cell Infect Microbiol* **10:** 581974.

Ershun, Z., Yunhe, F., Zhengkai, W., Yongguo, C., Naisheng, Z., and Zhengtao, Y. (2014) Cepharanthine attenuates lipopolysaccharide-induced mice mastitis by suppressing the NF-κB signaling pathway. *Inflammation* **37:** 331–337.

Feuerstein, J.D., Isaacs, K.L., Schneider, Y., Siddique, S.M., Falck-Ytter, Y., Singh, S., *et al.* (2020) AGA clinical practice guidelines on the management of moderate to severe ulcerative colitis. *Gastroenterology* **158:** 1450–1461.

Fu, X., Sun, F., Wang, F., Zhang, J., Zheng, B., Zhong, J., *et al.* (2017) Aloperine protects mice against DSS-induced colitis by PP2A-mediated PI3K/Akt/mTOR signaling suppression. *Mediators Inflamm* **2017:** 5706152.

Grant, C.V., Loman, B.R., Bailey, M.T., and Pyter, L.M. (2021) Manipulations of the gut microbiome alter chemotherapy-induced inflammation and behavioral side effects in female mice. *Brain Behav Immun* **95:** 401–412.

He, J., Song, Y., Li, G., Xiao, P., Liu, Y., Xue, Y., *et al.* (2019) Fbxw7 increases CCL2/7 in CX3CR1hi macrophages to promote intestinal inflammation. *J Clin Invest* **129:** 3877–3893.

Hifumi, T., Yamamoto, A., Morokuma, K., Okada, I., Kiriu, N., Ogasawara, T., *et al.* (2013) Clinical efficacy of antivenom and cepharanthine for the treatment of Mamushi (*Gloydius blomhoffii*) bites in tertiary care centers in Japan. *Jpn J Infect Dis* **66:** 26–31.

Hold, G., Smith, M., Grange, C., Watt, E., El-Omar, E., and Mukhopadhya, I. (2014) Role of the gut microbiota in inflammatory bowel disease pathogenesis: what have we learnt in the past 10 years? *World J Gastroenterol* **20:** 1192–1210.

Hon, K.L., and Leung, A.K. (2011) Alopecia areata. *Recent Pat Inflamm Allergy Drug Discov* **5:** 98–107.

Hosomi, S., Oshitani, N., Kamata, N., Sogawa, M., Okazaki, H., Tanigawa, T., *et al.* (2011) Increased numbers of immature plasma cells in peripheral blood specifically overexpress chemokine receptor CXCR3 and CXCR4 in patients with ulcerative colitis. *Clin Exp Immunol* **163:** 215–224.

Huang, H., Hu, G., Wang, C., Xu, H., Chen, X., and Qian, A. (2014) Cepharanthine, an alkaloid from Stephania cepharantha Hayata, inhibits the inflammatory response in the RAW264.7 cell and mouse models. *Inflammation* **37:** 235–246.

Iijima, N., Mattei, L.M., and Iwasaki, A. (2011) Recruited inflammatory monocytes stimulate antiviral Th1 immunity in infected tissue. *Proc Natl Acad Sci USA* **108:** 284–289.

Imhann, F., Vich Vila, A., Bonder, M.J., Fu, J., Gevers, D., Visschedijk, M.C., *et al.* (2018) Interplay of host genetics and gut microbiota underlying the onset and clinical presentation of inflammatory bowel disease. *Gut* **67:** 108–119.

Jonkers, D., Penders, J., Masclee, A., and Pierik, M. (2012) Probiotics in the management of inflammatory bowel disease: a systematic review of intervention studies in adult patients. *Drugs* **72:** 803–823.

Kanamori, S., Hiraoka, M., Fukuhara, N., Oizumi, Y., Danjo, A., Nakata, K., *et al.* (2016) Clinical efficacy of cepharanthin(R)for radiotherapy-induced leukopenia – a nationwide, multicenter, and observational study. *Gan To Kagaku Ryoho* **43:** 1075–1079.

Kao, M.C., Yang, C.H., Sheu, J.R., and Huang, C.J. (2015) Cepharanthine mitigates pro-inflammatory cytokine response in lung injury induced by hemorrhagic shock/resuscitation in rats. *Cytokine* **76:** 442–448.

Li, C., Ai, G., Wang, Y., Lu, Q., Luo, C., Tan, L., *et al.* (2020) Oxyberberine, a novel gut microbiota-mediated metabolite of berberine, possesses superior anti-colitis effect: Impact on intestinal epithelial barrier, gut microbiota profile and TLR4-MyD88-NF-kappaB pathway. *Pharmacol Res* **152:** 104603.

Liang, Y.-N., Yu, J.-G., Zhang, D.-B., Zhang, Z., Ren, L.-L., Li, L.-H., *et al.* (2019) Indigo naturalis ameliorates dextran sulfate sodium-induced colitis in mice by modulating the intestinal microbiota community. *Molecules* **24:** 4086.

Marchesi, J.R., Adams, D.H., Fava, F., Hermes, G.D.A., Hirschfield, G.M., Hold, G., *et al.* (2016) The gut microbiota and host health: a new clinical frontier. *Gut* **65:** 330–339.

Rakoff-Nahoum, S., Paglino, J., Eslami-Varzaneh, F., Edberg, S., and Medzhitov, R. (2004) Recognition of commensal microflora by toll-like receptors is required for intestinal homeostasis. *Cell* **118:** 229–241.

Semwal, D.K., Badoni, R., Semwal, R., Kothiyal, S.K., Singh, G.J., and Rawat, U. (2010) The genus Stephania (Menispermaceae): chemical and pharmacological perspectives. *J Ethnopharmacol* **132:** 369–383.

Shahriyar, S.A., Woo, S.M., Seo, S.U., Min, K.J., and Kwon, T.K. (2018) Cepharanthine enhances TRAIL-mediated apoptosis through STAMBPL1-mediated downregulation of survivin expression in renal carcinoma cells. *Int J Mol Sci* **19:** 3280.

Shen, S.J., Prame Kumar, K., Stanley, D., Moore, R.J., Van, T.T.H., Wen, S.W., *et al.* (2018) Invariant natural killer T cells shape the gut microbiota and regulate neutrophil recruitment and function during intestinal inflammation. *Front Immunol* **9:** 999.

Ungaro, R., Mehandru, S., Allen, P.B., Peyrin-Biroulet, L., and Colombel, J.F. (2017) Ulcerative colitis. *Lancet* **389:** 1756–1770.

Wen, X., Wang, H.G., Zhang, M.N., Zhang, M.H., Wang, H., and Yang, X.Z. (2021) Fecal microbiota transplantation ameliorates experimental colitis via gut microbiota and T-cell modulation. *World J Gastroenterol* **27:** 2834–2849.

Wu, X., Guo, Y., Min, X., Pei, L., and Chen, X. (2018) Neferine, a bisbenzylisoquinoline alkaloid, ameliorates dextran sulfate sodium-induced ulcerative colitis. *Am J Chin Med* **46:** 1263–1279.

Wu, Z., Pan, D., Jiang, M., Sang, L., and Chang, B. (2021) Selenium-enriched lactobacillus acidophilus ameliorates dextran sulfate sodium-induced chronic colitis in mice by regulating inflammatory cytokines and intestinal microbiota. *Front Med (Lausanne)* **8:** 716816.

Xiong, X., Cheng, Z., Wu, F., Hu, M., Liu, Z., Dong, R., and Chen, G. (2021) Berberine in the treatment of ulcerative colitis: a possible pathway through Tuft cells. *Biomed Pharmacother* **134:** 111129.

Yamazaki, T., Shibuya, A., Ishii, S., Miura, N., Ohtake, A., Sasaki, N., *et al.* (2017) High-dose Cepharanthin for pediatric chronic immune thrombocytopenia in Japan. *Pediatr Int* **59:** 303–308.

Zhang, X., Li, C., Cao, W., and Zhang, Z. (2021) Alterations of gastric microbiota in gastric cancer and precancerous stages. *Front Cell Infect Microbiol* **11:** 559148.

Zhang, X.-J., Yuan, Z.-W., Qu, C., Yu, X.-T., Huang, T., Chen, P.V., *et al.* (2018) Palmatine ameliorated murine colitis by suppressing tryptophan metabolism and regulating gut microbiota. *Pharmacol Res* **137:** 34–46.

Zhao, J., Piao, X., Wu, Y., Liang, S., Han, F., Liang, Q., *et al.* (2020) Cepharanthine attenuates cerebral ischemia/reperfusion injury by reducing NLRP3 inflammasome-induced inflammation and oxidative stress via inhibiting 12/15-LOX signaling. *Biomed Pharmacother* **127:** 110151.

Zheng, S., Zhu, Y., Wu, W., Zhang, Q., Wang, Y., Wang, Z., and Yang, F. (2021) A correlation study of intestinal microflora and first-episode depression in Chinese patients and healthy volunteers. *Brain Behav* **11:** e02036.

Zhou, P., Li, Z., Xu, D., Wang, Y., Bai, Q.I., Feng, Y., *et al.* (2019) Cepharanthine hydrochloride improves cisplatin chemotherapy and enhances immunity by regulating intestinal microbes in mice. *Front Cell Infect Microbiol* **9:** 225.

Supporting information

Additional supporting information may be found online in the Supporting Information section at the end of the article.

Fig. S1. Effects of CEP-only treatment on mice.

Fig. S2. mRNA expression of genes in the colon tissue.

Table S1. Primers for RT-PCR analysis.